19

Tactile Sensing and Tactile Imaging in Detection of Cancer

A. Sarvazyan, V. Egorov, and N. Sarvazyan

CONTENTS

19.1 Introduction

19.1.1 Background of Tactile Imaging Technology

Since Hippocrates, the human sense of touch has been the most prevalent and successful medical diagnostic technique. A great variety of diseases were diagnosed through tactile sensing including detection of malignant tumors. Hippocrates in 400 B.C. wrote as follows: "… Such swellings as are soft, free from pain, and yield to the finger, … and are less dangerous than the others. … then, as are painful, hard, and large, indicate danger of speedy death; but such as are soft, free of pain, and yield when pressed with the finger, are more chronic than these…" [28].

    In ancient medicine, medical practitioners have used diagnostic methods based on assessment of mechanical properties of tissues for diagnosing and treating ailments without much help from other tests. During the last century, traditional physical examination techniques were becoming outmoded and were often considered of little clinical value in comparison with many other modern diagnostic technologies. Palpation is only briefly addressed in medical school, and few physicians have the tactile ability to detect subtle variations of tissue elasticity. Few physicians are willing to devote the necessary time to master the technique, despite the fact that the American Cancer Society guidelines suggest for women that clinical breast examination (CBE) be part of a periodic health examination [1] and the American Urological Association in their 2009 Best Practices Statement recommended that men who wish to be screened for prostate cancer should have both a prostate-specific antigen (PSA) test and a digital rectal examination (DRE) [2].

    The development of modern diagnostic technologies has brought a decline in physical examination skills. But is this technique on the way to extinction? During the last two decades, several devices

AQ1

were developed which mimicked both the tactile sensors and the analysis part of traditional palpation techniques; many experimental and theoretical papers were published and patents filed. Numerous emerging technologies, such as various version of ultrasound and MR elasticity imaging, started to bring new life into the ancient technique of diagnostics based on assessment of tissue mechanical properties: *Le Roi Est Mort, Vive Le Roi!*

The task of developing tactile sensors fully mimicking the human fingertip and the mechanism of transduction of the tactile sensor stimuli into nerves and further analysis by brain is extremely diffi-cult because Mother Nature created sophisticated and highly sensitive system for obtaining information through sense of touch. A tactile sensing system of a human uses sensory information derived from mechanoreceptors embedded in the skin to provide data from an area contacting with an object and from mechanoreceptors rooted in muscles, tendons, and joints to provide motion tracking data [37]. Each fingertip is equipped with about 2000 tactile sensors [31] located inside two major layers of the skin (epi-dermis and dermis) and the underlying subcutaneous tissue. These layers have the four mechanorecep-tor populations: Meissner corpuscles, Merkel cell neurite complexes, Pacinian corpuscles, and Ruffini endings. Primary functions of each mechanoreceptor population are found to be different. They provide texture perception, pattern and form detection, motion detection, stable precision grasp, and manipula-tion [80]. Average applied pressure differential sensitivity for human fingertips was found to be about 900 Pa [34]. The tactile spatial resolution is within the range from 0.8 to 1.6 mm [9,22,67]. The temporal resolution of human tactile sensing is about 0.05 s as measured between successive taps on the skin [21]. The tactile roughness sensitivity of human fingertip is typically about 0.2 mm [6], but may reach up to 0.02 mm [41].

However, manual palpation aiming at cancer detection, such as CBE or DRE, makes use of only a small fraction of plurality of the fingertip tactile system features. This makes the task of developing a diagnostic technology mimicking the sophisticated means implemented by Mother Nature in the human fingertip much more realistic.

19.1.2 Emergence of Tactile Imaging

The first description of a technical implementation related to tactile imaging (TI) was given in the late 1970s by Frei et al. [18,19] who proposed an instrument for breast palpation that used a plurality of spaced piezoelectric force sensors. The sensors were pressed against the breast tissue by a pressure mem-ber which applied a given periodic or steady stress to the tissue. A different principle for evaluating the pattern of pressure distribution over a compressed breast was proposed by Gentle [20] 8 years later. The pressure distribution was monitored optically by using the principle of frustrated total internal reflection to generate a brightness distribution (see Figure 19.1). Using this technique, simulated lumps in breast prostheses were detected down to a diameter of 6 mm. But the author was unable to obtain any quantita-tive data on lumps in a real breast. The failure has been explained by the insufficient sensitivity of the registration system and that "the load, that the volunteers could comfortably tolerate, was less than that used in the simulation." Then, Sabatini et al. built a robotic system for discriminating mechanical inho-mogeneities in a soft tissue using a finger-like palpation device equipped with a fingertip piezoelectric polymer film tactile sensor [57].

TI as a modality of medical diagnostics based on reconstruction of tissue structure and elastic proper-ties using mechanical sensors was introduced in the 1990s by Sarvazyan et al. in Artann Laboratories [58,63] and by Wellman et al. in Harvard University [76,77]. TI, which is also called "mechanical imaging" or "stress imaging," is most closely mimicking manual palpation because the TI probe with a pressure sensor array mounted on its tip acts similar to human fingers during clinical examination, slightly compressing soft tissue by the probe. In essence, TI "captures the sense of touch" and stores it permanently in digital format for analysis and comparison. Extensive laboratory studies on breast phan-toms and excised prostates have shown that the computerized palpation is more sensitive than human finger [14,59,79].

The TI examination is performed through a set of manual compressions of the target tissue/organ by pressure sensor array mounted on a hand-held probe. The pressure response pattern shows spatial dis-tribution of softer and harder areas of the palpated region, thus providing information on the presence,
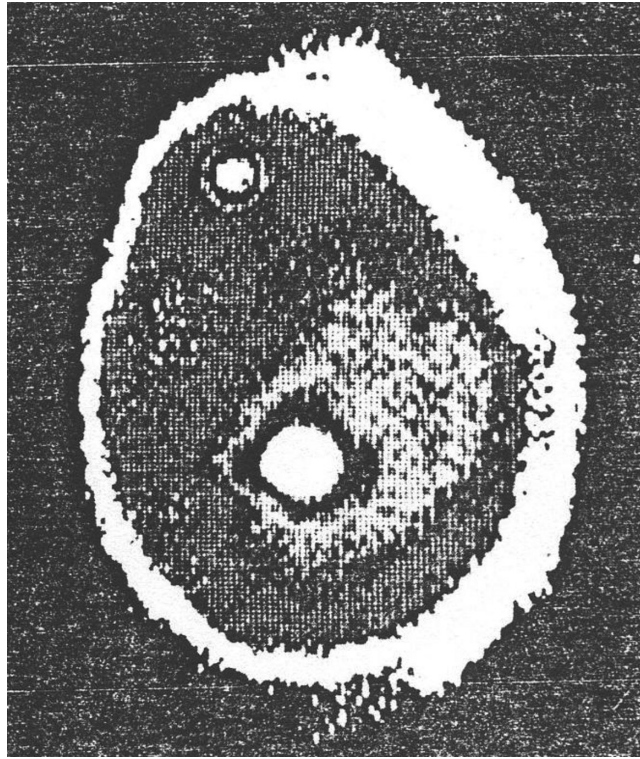
FIGURE 19.1 On one of the first elastographic images published in 1988, a stress pattern recorded on the surface of compressed breast phantom (rubber prosthesis filled with silicone rubber gel) containing two lumps (nylon balls of diameters 25 and 6 mm). (Reproduced from Gentle, C.R., *J. Biomed. Eng.,* 10, 124, 1988. With permission.)

dimensions, and location of hard inclusions. Stress profile resulting from the presence of a hard nodule strongly depends on the nodule shape, size, hardness, and depth.

During the last decade, TI was implemented in several devices for a variety of applications. These devices included the prostate mechanical imager (PMI) for 3-D prostate visualization highlighting prostate nodularity in terms of tissue elasticity [13,78], the breast mechanical imager for breast cancer detection [14], and the vaginal tactile imager for pelvic organ prolapse assessment [16].

19.1.3 Sensors for Tactile Imaging

A wide variety of technologies, optical, electromechanical, and ultrasonic, have been explored to address the tactile sensing problem in robotics and medicine [73]. Most of the sensors and transduction mechanisms tested in applications related to TI, such as capacitive, resistive, based on piezopolymers, fiber optics, conductive elastomers, and MEMS sensors, appeared to be far from optimal due to either insufficient sensitivity and reproducibility, excessive hysteresis, or fast aging [4,5,8,25,38,39,42,55,56].

The TI devices developed in the 1990s [44,76] employed Tekscan resistive pressure sensor array (Boston, MA) [55]. Tekscan sensor is based on changing electrical resistance under external pressure of electroconductive powder layer embedded between two flexible polyester sheets. The main drawback of Tekscan sensors limiting their applicability in TI applications is low reproducibility and fast aging.

The other type of sensor arrays which satisfied the requirements of TI and which is currently implemented in the TI systems appeared to be the capacitive tactile sensors developed by Pressure Profile Systems, Inc. (PPS), Los Angeles, CA [71]. The PPS sensor array is a capacitor grid produced by a set of orthogonal electrodes. The basic technical characteristics for PPS sensors are as follows: basic

operational range is 0–60 kPa, noise level/sensitivity 0.06 kPa, reproducibility 0.8 kPa, and temperature sensitivity 0.05 kPa/°C. These characteristics fully correspond to the requirements of TI technology.

19.1.4 Potential of Tactile Imaging for Detecting Cancer

The very first clinical study on the application of TI technology for cancer detection was conducted on excised prostate glands in 1998 [44,45]. Seven radical prostatectomy and two cystoprostatectomy specimens were evaluated by a proof-of-concept TI prototype with a Tekscan sensor array. Excised prostates were placed with the posterior side facing down on 110 mm × 110 mm sensor array. Manual pressure was applied to the prostate anterior surface for 3–5 s to produce 300–500 tactile images of the gland. The prostates were further histopathologically analyzed for the presence of cancer. The results of the mechanical imaging and pathological analysis were closely correlated. Figure 19.2 provides an example illustrating the results of that study.

Mechanical properties of tissues are highly sensitive to the structural changes accompanying various physiological and pathological processes. A change in Young's modulus of tissue during the development of a tumor could reach thousands of percent [64,76]. Evaluation of tissue "hardness" (Young's or shear elasticity modulus) by various elasticity imaging techniques provides means for characterizing the tissue, differentiating normal and diseased conditions, and detecting tumors and other lesions [60]. Tumors or tissue blocked from its blood nutrients is stiffer than normal tissue. Further, benign and cancerous tumors have distinguishing elastic properties [35,70].

Over the last two decades, there has been significant development in different methods to visualize mechanical structure of tissues in terms of their elasticity properties. Every elasticity imaging method involves two common elements: the application of a force and the measurement of a mechanical response. The measurement method can be performed using differing physical principles including magnetic resonance imaging (MRI) [17,43,52,68] and ultrasound imaging [46,47,50,64,65]. TI is a branch of elasticity imaging; it differs from conventional ultrasonic and MR elasticity imaging in that it evaluates soft tissue mechanical structure using stress data rather than dynamic or static strain data.

The current surge of publications on ultrasonic and MR elasticity imaging covers practically all key human organs [61]. Researchers from numerous laboratories all over the world demonstrated the potential of elasticity imaging in cancer diagnostics and differentiating benign and malignant lesions. Table 19.1 illustrates the sensitivity and specificity of elasticity imaging in differentiating benign vs. malignant lesions using literature data on assessment of breast cancer by various elasticity imaging modalities: USE (ultrasound elastography), MRE (magnetic resonance elastography), and TI. These data show that elasticity imaging even in its least sophisticated version, like TI, has significant diagnostic potential comparable and exceeding that of conventional imaging techniques such as mammography, MRI, and ultrasound. Results of clinical studies indicate that TI has a potential not only to just detect tumors but also to distinguish between benign and malignant classes of fibroadenoma, cyst, fibrosis, ductal, lobular carcinoma, and other conditions [15].
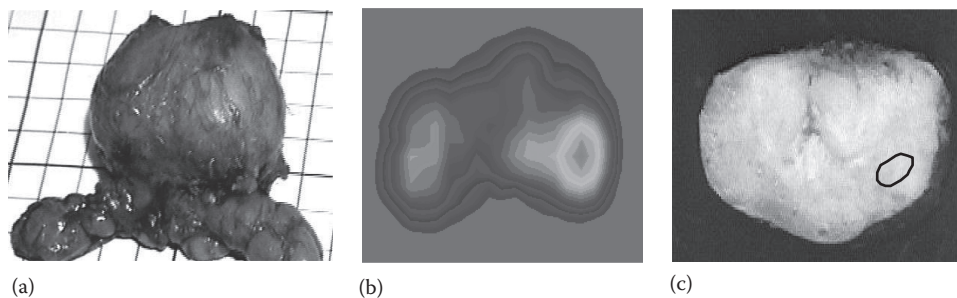

(a)   (b)   (c)

FIGURE 19.2   An excised prostate (a), its mechanical image (b), and corresponding pathology section (c) revealing a cancerous nodule (adenocarcinoma with Gleason score 4) at the location exactly corresponding to that on the mechanical image. (Adapted from Niemczyk, P. et al., *J. Urol*. 160, 797, 1998. With permission.)

TABLE 19.1

Recent Clinical Data on Benign-Malignant Breast Lesion Differentiation by Elasticity Imaging

No.	Method	Number of Analyzed Lesions	Sensitivity (%)	Specificity (%)	Citation
1	USE	52 malignant/59 benign	86.5	89.8	Itoh et al. [29]
2	USE	49 malignant/59 benign	91.8	91.5	Thomas et al. [74]
3	MRE	38 malignant/30 benign	95.0	80.0	Sinkus et al. [69]
4	USE	50 malignant/48 benign	99.3	25.7	Burnside et al. [11]
5	USE	237 malignant/584 benign	97.5	48.0	Svensson et al. [72]
6	TI	32 malignant/147 benign	91.4	86.1	Egorov et al. [15]
7	SSI	82 malignant/110 benign	87.8	87.3	Cosgrove et al. [12]
8	USE	144 malignant/415 benign	92.4	91.1	Zhi et al. [82]
9	USE	61 malignant/127 benign	92.7	85.8	Raza et al. [54]

USE, ultrasound elastography; MRE, magnetic resonance elastography. TI, tactile imaging; SSI, supersonic shear imaging.

19.2 Materials and Methods

Several devices have been developed based on the TI technology for detection and 3-D visualization of cancer. General architecture of these devices has several common features and components, such as a probe with an array of tactile sensors, an electronic unit, and a touch screen laptop computer [13,14]. The configuration of the probe, structure of sensors, user interface, and data processing algorithms are specific for a particular application. Figures 19.3 and 19.4 show general view of the devices for breast (Medical Tactile, CA) and prostate TI (Artann Laboratories, NJ; ProUroCare Medical, MN). The probe for the tactile breast imager (TBI) has a pressure sensor array of 40 mm by 30 mm comprising 192 pressure sensors to acquire pressure patterns between the probe surface and the exterior skin layer of the breast during contact (Figure 19.3). Each pressure sensor has rectangular pressure sensing area of 2.5 mm by 2.0 mm (PPS, CA).
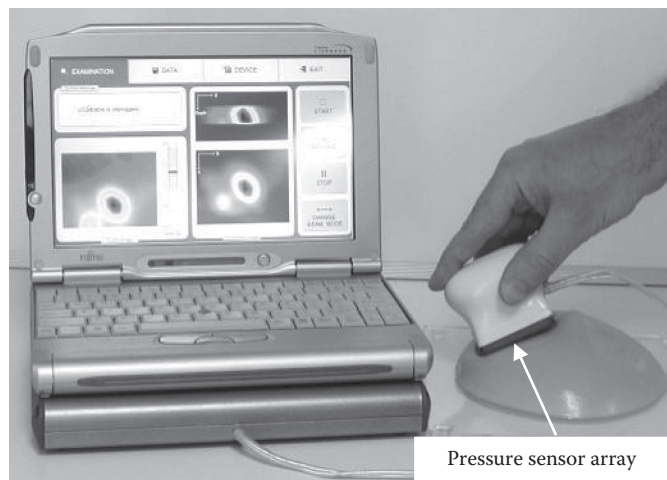

Pressure sensor array

FIGURE 19.3 General view of the TBI. The device comprises a probe with 2-D pressure sensor array, an electronic unit, and a laptop computer with touch screen capability. (Reproduced from Egorov, V. and Sarvazyan, A.P., *IEEE Trans. Med. Imaging,* 27, 1275, 2008. With permission.)
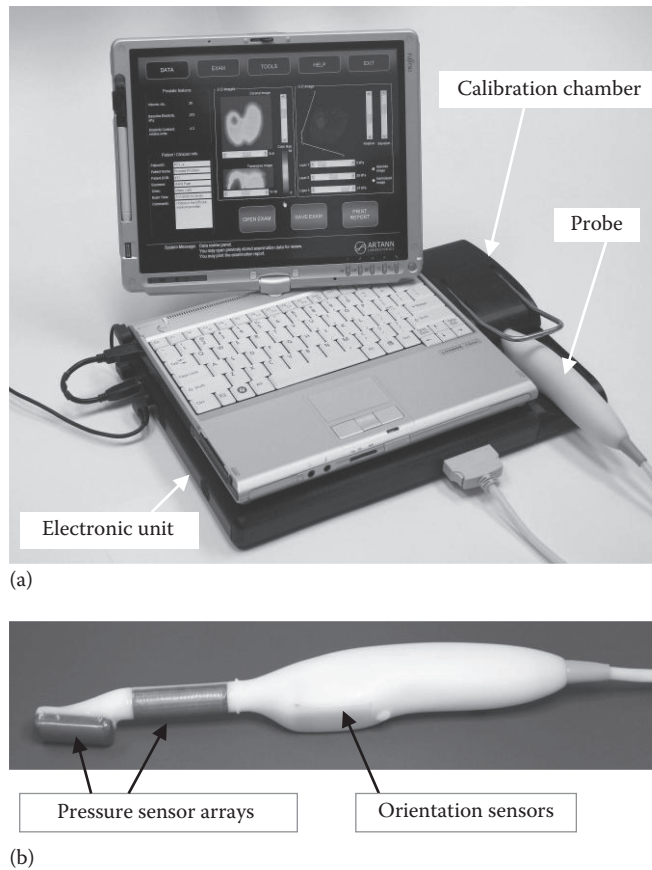
(a)

(b)

FIGURE 19.4 The prostate mechanical imaging system. (a) General view of the system; (b) transrectal probe.

The transrectal probe of the PMI is much more complex. It comprises two separate pressure sensor arrays and orientation sensors. The first pressure sensor array is installed on the probe head surface, and it is in contact with prostate through the rectal wall during the examination procedure. The second pressure sensor array is installed on the probe shaft surface for assessment of the pressure pattern in the sphincter area during the manipulation of the probe. The probe shaft and head pressure arrays differ by their geometry and sensor's size. The probe head pressure sensor array comprises 128 (16×8) pressure sensors covering an area of 40 mm by 16 mm while the shaft sensor array comprises 48 sensors (16×3), and the sensors have different dimensions ($3.75\,mm \times 2.5\,mm$). In contrast to the TBI probe, the PMI probe includes also an orientation system (InterSense, Inc., MA) mounted in the probe handle. The probe head pressure sensors are intended for acquisition prostate pressure patterns as well as for calcula-tion of the possible prostate displacements during probe head pressing against the prostate. The probe shaft pressure sensors are capturing and tracking the sphincter position that allows real-time spatial visualization of the sphincter and prostate area to help an operator in finding the prostate and assist in probe manipulation. Another important function of the probe shaft sensor array is to provide quantitative information on the level of forces exerted by the operator on the sphincter. Displaying this information on the user interface helps the operator to avoid excessive stretching of patient's sphincter, which is one of the causes of patient's discomfort during examination. Calculated distance between the sphincter and prostate and the probe azimuth angle helps to compute left/right probe head displacement relative to a start reference line.

During the examination of the breast with TBI, the patient is placed in a position similar to that of a standard CBE with her breast in the supine position on a standard examination table. The examiner

places a disposable sheath over the sensor head of the TBI and then applies a water soluble lubricating lotion to the sensor head or applied directly to the area of concern. The examination is recorded and stored by the TBI system in a digital format file. The duration of a typical lesion scan is approximately 1–2 min.

For the PMI examination, a patient is asked to bend over the examination table so as to form a 90° angle at the waist. The patient places his chest on a table, so that his weight is applied to the table surface in order to free leg muscles from tension. The rectum does not need to be evacuated prior to the examination. A lubricated probe is inserted into the rectum with the probe head sensor surface down until the prostate is visualized on the computer. The prostate scan is performed through a set of multiple compressions. The examiner is able to see in real time two orthogonal prostate cross sections with the relative location of the probe head pressure-sensitive area in both projections. The PMI scan takes 40–60 s on average, and the collected data are saved in a digital format.

Software of tactile imagers allows real-time visualization and 2-D/3-D computer-aided reconstruction of the examined tissue and detected abnormalities. An operator may look through various orthogonal slices of the examined tissue. The software also offers a standard range of data management features, such as data storage and retrieval and image printout. An additional set of image enhancement techniques are applied to improve the image, data acquisition, and lesion detection, as illustrated in Figure 19.5 [14,15]. Image enhancement techniques such as low-pass noise filtration, signal thresholding and 2-D interpolation, pixel neighborhood rating–based filtering, and 2-D interpolation are used to increase signal-to-noise ratio. Assessment of the motion of lesions relative to probe sensing surface is performed to identify the mobility of lesions, an important diagnostic feature. The 2-D image matching is performed to generate a compound image from a sequence of successive images obtained along the scanning trajectory over the detected lesion. Lastly, geometrical characteristics of the detected lesions, including lesion shape, edges, strain hardening, mobility as an ability to change shape, and position under applied stress are calculated.

An important feature of TI is the ability of 3-D reconstruction of internal structures using data of stress patterns on the surface of the examined tissue at different levels of compression (Figure 19.6). The input data for 3-D reconstruction comprise a continuous sequence of 2-D filtered images. The initial hypotheses enabling 3-D reconstruction are as follows: (a) the higher the compression force, the greater the representation of deeper structures in the imprint image and (b) the total pressure is proportional to the tissue deformation in the direction normal to the probe surface (Z-axis). The 3-D reconstruction starts with the formation of an initial (seed) 3-D structure by stacking the series of 2-D structure images along Z-axis during first tissue compression. Every 2-D imprint is further integrated by a parallel translation inside the 3-D structure image by a matching algorithm [14]. The final 3-D structure visualization
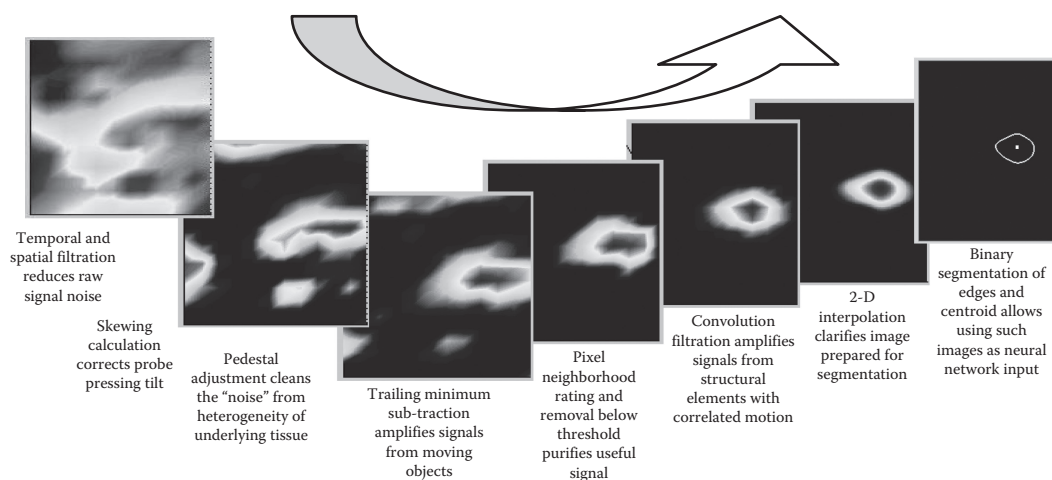

Temporal and spatial filtration reduces raw signal noise

Skewing calculation corrects probe pressing tilt

Pedestal adjustment cleans the "noise" from heterogeneity of underlying tissue

Trailing minimum sub-traction amplifies signals from moving objects

Pixel neighborhood rating and removal below threshold purifies useful signal

Convolution filtration amplifies signals from structural elements with correlated motion

2-D interpolation clarifies image prepared for segmentation

Binary segmentation of edges and centroid allows using such images as neural network input

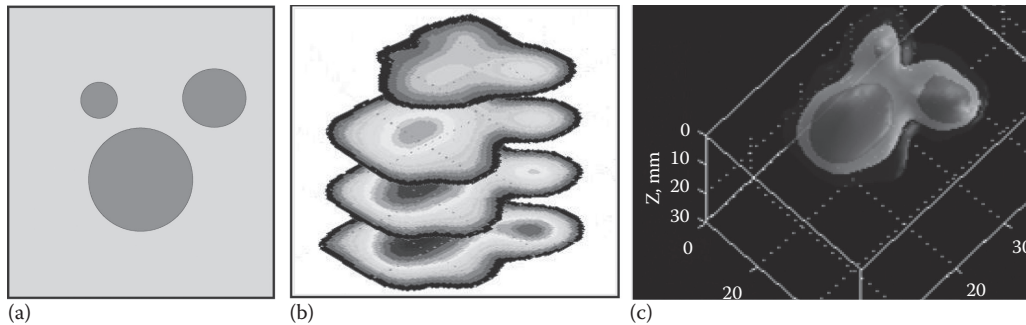**FIGURE 19.5** A sequence of algorithms for isolating the lesion signal while rejecting artifacts.

FIGURE 19.6 Illustration of an algorithm for 3-D image reconstruction. (a) Schematic top view of a test phantom (E=8 kPa) with three inclusions (E=125 kPa, D1=15 mm, D2=8 mm, and D3=5 mm) located at about 8 mm depth, (b) sequence of 2-D stress patterns obtained at different levels of compression, and (c) reconstructed 3-D image. See text for details.

is deployed by the computation of isosurfaces and 2-D image slices for the 3-D pressure field, which is related to the hardness distribution of the underlying structure. Figure 19.6 presents an example of the 3-D image reconstruction of a composite inclusion in the test phantom. Panel C in Figure 19.6 shows a composite inclusion visualized by means of three semitransparent isosurfaces (blue, green, and red). Each surface represents points of a constant value of pressure (10 kPa, 17 kPa, and 25 kPa, respectively) in 3-D space. The relative elasticity levels forming 2-D image slices (panel B in Figure 19.6) are represented by a color map. The colors from blue to red are selected to provide a visual demarcation between different levels of pressure response. The blue color corresponds to the lowest level, and red corresponds to the highest level of the pressure response. The ability of this approach to reproduce the underlying tissue structures was demonstrated on a variety of phantom models and clinical data [13,14,78].
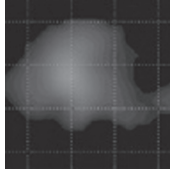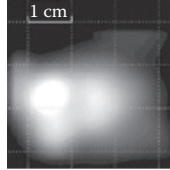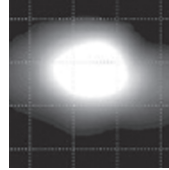
19.3 Results

The results of clinical testing of various TBI and PMI prototypes are described in several publications [15,26,78,79]. Here we will show some representative results illustrating the potential of the TI technology in cancer detection.
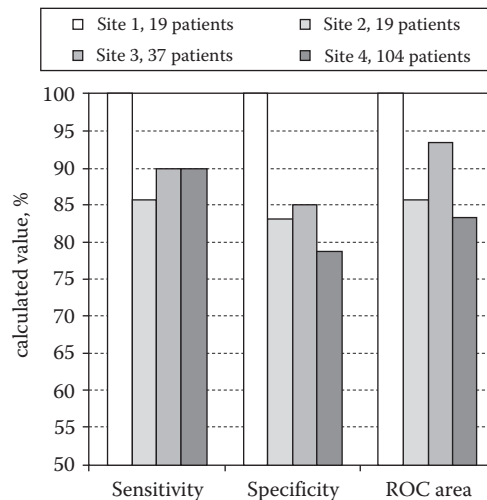
19.3.1 Tactile Imaging of Breast

There were several clinical studies performed on diagnostic/screening potential of breast TI. In one clinical study that included 110 patients with a complaint of a breast mass, TI demonstrated detection of 94% of the breast mass, while CBE identified only 86% [32]. The positive predictive value for breast cancer using TI was 94%. Another study with 179 patients (147 benign and 32 malignant cases) was conducted at four clinical sites to evaluate the TBI capability for breast lesion characterization and differentiation [15]. Tissue biopsy data were used as a gold standard in tissue differentiation. Examples of actual tactile images of breast lesions are shown in Table 19.2. Five features of the detected lesions were calculated from the acquired pressure pattern data for breast lesion characterization: strain hardening (F1), loading curve average slope (F2), maximum pressure peak for the fixed total force applied to the probe (F3), lesion shape (F4), and lesion mobility (F5) [15]. All these features (F1–F5) plus a patient age (F6) were used as input data of a Bayesian classifier to calculate probability of lesion being benign P(b) and malignant P(m) for a given set of input features. Clinical examples of calculated features for detected lesions from the acquired pressure pattern data for breast lesion are presented in Table 19.2. The difference between P(b) and P(m) was used as a threshold parameter for the construction of the receiver operating characteristic (ROC) curve to analyze the ability of the TBI in differentiation of benign from malignant lesions. The area under the ROC curve (AUC) demonstrating the diagnostic accuracy in discrimination of benign

TABLE 19.2

Clinical Examples of Breast Lesion Imaging and Feature Calculations

Case number, patient ID	1, L13	2, S27	3, S24
Patient age (F6)	55	25	54
Lesion biopsy diagnosis	Benign (fibrosis)	Benign (fibroadenoma)	Malignant (ductal carcinoma)
Breast lesion image			
Calculated features			
Strain hardening (F1), rel. units	−5.4	22.9	20.9
Loading slope (F2), rel. units	6.1	14.4	17.7
Peak pressure (F3), kPa	4.7	18.0	32.4
Lesion shape (F4), %	128	117	106
Lesion mobility (F5), %	44	12	11
Classifier output, P(b)–P(m)	0.72	0.13	−0.51

FIGURE 19.7 Differentiation for benign and malignant lesions with the use of Bayesian classifier evaluated for four clinical sites. (From Egorov, V. et al., *Breast Cancer Res. Treat.,* 118, 67, 2009.)

and malignant lesions was calculated separately for each clinical site. Figure 19.7 presents the calculated sensitivity, specificity, and AUC for each clinical site. We found that the sensitivity ranges from 85.7% to 100%, specificity from 78.7% to 100%, and AUC from 83.4% to 100%. An average sensitivity of 91.4% and a specificity of 86.8% with a standard deviation of ±6.1% were found. For clinical data combined from all sites, the AUC was equal to 86.1% with the 95% confidence interval (CI) from 80.3% to 90.9% while a significance level P=0.0001 for the area of 50%; sensitivity was equal to 87.5% with the 95% CI from 71.0% to 96.4%±12% (95% CI) and specificity 84.4% with the 95% CI from 77.5% to 89.8% [15].

19.3.2 Tactile Imaging of Prostate

Capability of PMI technology to provide an objective image of the prostate and detect abnormalities was evaluated in a clinical setting. Figure 19.8 illustrates clinical examples of healthy and two prostate
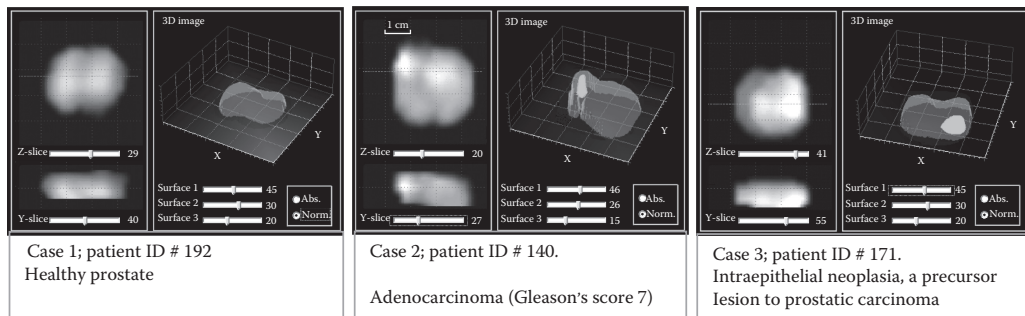
FIGURE 19.8 Examples of MI examination results. Left panel shows 2-D and 3-D mechanical images of a normal prostate, and two following panels show images of diseased prostates.
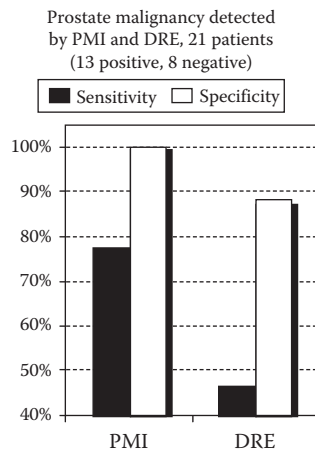

FIGURE 19.9 Malignancy detection by PMI vs. biopsy and DRE vs. biopsy.

pathology cases as were diagnosed by the transrectal ultrasound (TRUS)-guided biopsy. PMI 2-D coronal and transverse images (the top and bottom 2-D patterns, respectively) and a composite 3-D image of the prostate gland clearly visualize the prostate and confirm presence of hard nodules [78].

The ROC analysis was conducted on the clinical study sample of 168 subjects to demonstrate the ability of the PMI to visualize nodules. The AUC was calculated to be 81%, with a 95% CI from 74% to 88%. The subgroup of the study was referred for further TRUS-guided biopsy testing as a result of patients having an elevated PSA level above 4.0 ng/mL, an abnormal DRE finding, or a combination of age or family prostate cancer history factors. For 13 patients in the study (PSA levels ranging from 1.0 to 26.7 ng/mL) with the presence of cancerous nodules confirmed by biopsy, PMI confirmed the biopsy results for 10 of the 13 cancer patients. The DRE identified only 6 of the 13. In the 8 cases (PSA levels ranging from 4.4 to 13.6 ng/mL) that were defined by the TRUS-guided biopsy as noncancerous, PMI depicted all 8 as normal images of the prostate, whereas the DRE detected 7 normal and 1 suspicious reading [78]. Figure 19.9 summarizes these findings and presents sensitivity and specificity for malignancy detection by PMI vs. biopsy and DRE vs. biopsy for a limited number of patients.

19.4 Discussion

Availability of health care is limited by its skyrocketing cost, and application of new advanced techniques frequently contributes to this escalation. Substantial disparity between industrialized countries and the rest of the world widens with more than 70% of all cancer deaths occurring in lower income

TABLE 19.3

Comparative Data for Breast Cancer Detection Effectiveness and Cost-Effectiveness

Screening/Diagnostic Technique	Sensitivity/Specificity, %	Procedure Cost of Bilateral Exam, USD	Cost-Effectiveness, USD per Life Year Gained
CBE	56.5/93.7	—	522, India [10]
			31,900, Japan [48]
Mammography	73.7/94.3	112[a]	1,846, India [10]
			26,500–331,000 [75]
Ultrasound	Limited, see text	70[a]	—
MRI	87.7/92.8	1037[a]	55,420–130,695 [66]
Biopsy	96.6/100.0	2061[b]	2,250–77,500 [23,27]
TI	91.9[d]/88.9	5–50[c]	162[c]

Source: Adapted from Sarvazyan, A.P. et al., *Breast Cancer Basic Clin. Res.*, 1, 91, 2008. With permission.

[a] The U.S. average Medicare reimbursements in 2005.

[b] In average for one biopsy.

[c] Projections based on a physician's assistant performing the exam.

[d] Averaged for two clinical studies.

countries where availability of resources for diagnosis, prevention, and treatment of cancer is limited or nonexistent [3,36,81]. Introduction of cost-effective screening and diagnostic methods for cancer is especially important in the developing countries and lower income population all over the world having limited access to the sophisticated conventional devices.

Current methods of breast screening and diagnosis include breast self-examination (BSE), CBE, mammography, ultrasound, MRI, and biopsy. Table 19.3 presents a summary of breast cancer screening/diagnostic efficiency for various techniques, procedure cost, and cost-effectiveness numbers. Clinical results demonstrate that tactile elasticity imaging with a sensitivity of 91.9% and specificity of 88.9% has significant diagnostic potential comparable to that of conventional imaging techniques. Further, the ease-of-use, portability, and no-radiation position TI technology well for early detection, monitoring, and measurement of recurrence. In view of many countries with limited resources, effective yet less expensive modes of screening must be considered globally. The substantially lower TI procedure cost makes it, possibly, one method that has the potential to provide cost-effective breast cancer screening and diagnostics worldwide.

AQ2

Another way of increasing the cost-effectiveness is enhancing diagnostic efficacy of screening that would lead to the higher rate of cancer detection. In the United States alone, more than one million breast biopsies are performed annually following mammography findings, and approximately 80% of these findings are benign [24,40]. To evaluate possible impact of TBI supplementing standard screening procedures (mammography alone or combination of mammography and conventional ultrasound) on the benign biopsy rate, one could apply TBI cancer sensitivity and specificity to the patient sample referred for the breast biopsy (20% malignant and 80% benign). The results signal that a 23% reduction of the benign biopsy is possible without missing cancer cases, while a 50% reduction of the benign biopsy with 4.6% missed cancer cases [15].

In case of the prostate cancer, frequently indolent and slow-progressing disease, adverse outcomes of overdiagnosis and overtreatment are weighted heavily against benefits of screening and early detection. In this context, active surveillance emerges as a new practical approach that provides for selective intervention on the individually defined need basis [33,49,51]. Introduction of a technology that could help discriminate between slow-growing and aggressive prostate tumors would be critical in guiding a curative treatment. PMI could augment PSA and ultrasound-guided biopsy by visual and quantitative assessment of changes in the mechanical properties of prostate tissue associated with disease progression. In addition, PMI imaging capability for visualization, recording, and tracking of the physical growth of the prostate nodule may significantly add to its diagnostic potential value. Another potential niche and clinical benefits of the use of PMI technology could be in expectant management. Such deferred treatment

involves actively monitoring the course of the disease with the expectation to intervene if the cancer progresses or if symptoms become imminent [7,30].

The limitations of TI in detecting tissue abnormality are close to that of a highly skilled physician: detection limit of superficial nodules is about 2–4 mm in diameter and larger nodules of 10–15 mm in diameter could be detected at a depth of no more than 40 mm. Further progress in TI technology is expected mainly in expanding its fields of applications. We believe that any area of medical diagnostics, where the sense of touch is shown to provide useful information on the state of a tissue or an organ, could become a new field of application of TI. In any such new application, e.g., examination of lymph nodes or detecting an abnormality in thyroid, the geometry of the TI probe must be carefully redesigned to conform to a particular examination site.

19.5 Conclusion

There is a tremendous worldwide need for cost-effective means to detect cancer at its earliest stage and to monitor it progression through treatment. TI, a comparatively low-cost, no-radiation, and easy-to-use technology, electronically and quantitatively captures cancer-induced transformation of the mechanical properties of soft tissues. The TI applications, including the TBI for breast and PMI for prostate, have the potential to be positioned as an adjunct to conventional methods leading to enhanced screening, reduced negative biopsy rates, and improved cancer detection.

ACKNOWLEDGMENT

REFERENCES

1. American Cancer Society. 2010. *Breast Cancer Facts & Figures 2009–2010*. Atlanta, GA: American Cancer Society, Inc.
2. American Urological Association. 2009. *Prostate-Specific Antigen Best Practice Statement: 2009 Update*. Linthicum, MD: Education and Research, Inc.
3. Anderson, B.O., R. Shyyan, A. Eniu, R.A. Smith, C.H. Yip, N.S. Bese, L.W. Chow, S. Masood, S.D. Ramsey, and R.W. Carlson. 2006. Breast cancer in limited-resource countries: An overview of the Breast Health Global Initiative 2005 guidelines. *Breast J*. **12**(Suppl.):S3–S15.
4. Beccai, L., S. Roccella, A. Arena, F. Valvoa, P. Valdastria, A. Menciassia, M.C. Carrozza, and P. Dario. 2005. Design and fabrication of a hybrid silicon three-axial force sensor for biomechanical applications. *Sens. Actuat. A Phys*. **120**:370–382.
5. Beebe, D.J., A.S. Hsieh, R.G. Radwin, and D.D. Denton. 1995. A silicon force sensor for robotics and medicine. *Sens. Actuat. A Phys*. **50**:55–65.
6. Bensmaïa, S.J. and M. Hollins. 2005. Pacinian representations of fine surface texture. *Percept. Psychophys*. **67**:842–854.
7. Bill-Axelson, A., L. Holmberg, M. Ruutu, M. Häggman, S.O. Andersson, S. Bratell, A. Spångberg, C. Busch, S. Nordling, H. Garmo, J. Palmgren, H.O. Adami, B.J. Norlén, J.E. Johansson, and Scandinavian Prostate Cancer Group Study No. 4. 2005. Radical prostatectomy versus watchful waiting in early prostate cancer. *New Eng. J. Med*. **352**:1977–1984.
8. Bloor, D., K. Donnely, K.J. Hands, P. Laughlin, and D. Lussey. 2005. A metal-polymer composite with unusual properties. *J. Phys. D Appl. Phys*. **38**:2851–2860.
9. van Boven, R. W., R. H. Hamilton, T. Kauffman, J.P. Keenan, and A. Pascual-Leone. 2000. Tactile spatial resolution in blind Braille readers. *Neurology* **54**:2230–2236.
10. Brown, M.L., S.J. Goldie, G. Draisma, J. Harford, and J. Lipscomb. 2006. Health service interventions for cancer control in developing countries. In D.T. Jamison, J.G. Breman et al. (eds.), *Disease Control Priorities in Developing Countries*, 2nd edn., Washington, DC: Oxford University Press, pp. 569–589.

11. Burnside, E.S., T.J. Hall, A.M. Sommer, G.K. Hesley, G.A. Sisney, W.E. Svensson, J.P. Fine, J. Jiang, and N.J. Hangiandreou. 2007. Differentiating benign from malignant solid breast masses with US strain imaging. *Radiology* **245**:401–410.

12. Cosgrove, D., C.J. Doré, C. Cohen-Bacrie, and J.P. Henry. 2010. Preliminary assessment of ShearWave(TM) elastography features in predicting breast lesion malignancy. *European Congress of Radiology*, Vienna, Austria. http://www.supersonicimagine.fr/fichiers/ts_etude/ecr2010_poster_c-0444_cosgrove.pdf

13. Egorov, V., S. Ayrapetyan, and A.P. Sarvazyan. 2006. Prostate mechanical imaging: 3-D image composition and feature calculations. *IEEE Trans. Med. Imaging* **25**:1329–1340.

14. Egorov, V. and A.P. Sarvazyan. 2008. Mechanical imaging of the breast. *IEEE Trans. Med. Imaging* **27**:1275–1287.

15. Egorov, V., T. Kearney, S.B. Pollak, C. Rohatgi, N. Sarvazyan, S. Airapetian, S. Browning, and A.P. Sarvazyan. 2009. Differentiation of benign and malignant breast lesions by mechanical imaging. *Breast Cancer Res. Treat*. **118**:67–80.

16. Egorov, V., H. van Raalte, and A.P. Sarvazyan. 2010. Vaginal tactile imaging. *IEEE Trans. Biomed. Eng*. **57**:1736–1744.

17. Fowlkes, J.B., S.Y. Emelianov, J.G. Pipe, A.R. Skovoroda, P.L. Carson, R.S. Adler, and A.P. Sarvazyan. 1995. Magnetic-resonance imaging techniques for detection of elasticity variation. *Med. Phys*. **22**:1771–1778.

18. Frei, E.H., B.D. Sollish, and S. Yerushalmi. March 1979. Instrument for viscoelastic measurement. U.S. patent 4,144,877.

19. Frei, E.H., B.D. Sollish, and S. Yerushalmi. February 1981. Instrument for viscoelastic measurement. U.S. patent 4,250,894.

20. Gentle, C.R. 1988. Mammobarography: A possible method of mass breast screening. *J. Biomed. Eng*. **10**:124–126.

21. Gescheider, G.A. 1974. Effects of signal probability on vibrotactile signal recognition. *Percept. Mot. Skills* **38**:15–23.

22. Grant, A.C., R. Fernandez, P. Shilian, E. Yanni, and M.A. Hill. 2006. Tactile spatial acuity differs between fingers: A study comparing two testing paradigms. *Percept. Psychophys*. **68**:1359–1362.

23. Groenewoud, J.H., R.M. Pijnappel, M.E. van den Akker-van Marle, E. Birnie, T. Buijs-van der Woude, W.P Mali, H.J. de Koning, and E. Buskens. 2004. Cost-effectiveness of stereotactic large-core needle biopsy for nonpalpable breast lesions compared to open-breast biopsy. *British J. Cancer* **90**:383–392.

24. Gur, D., L.P. Wallace, A.H. Klym, L.A. Hardesty, G.S. Abrams, R. Shah, and J.H. Sumkin. 2005. Trends in recall, biopsy, and positive biopsy rates for screening mammography in an academic practice. *Radiology* **235**:396–401.

25. Helsel, M., J.N. Zemel, and V. Dominko. 1988. An impedance tomographic tactile sensor. *Sens. Actuat. A Phys*. **14**:93–98.

26. Helvie, M.A., P.L. Carson, A.P. Sarvazyan, N. Thorson, V. Egorov, and M.A. Roubidoux. 2003. Mechanical imaging of the breast: A pilot trial. *Ultrasound Med. Biol*. **29**(Suppl.):S112.

27. Hillner, B.E. 2004. Cost and cost-effectiveness considerations. In J.R. Harris, M.E. Lipman, M. Mprrow, C.R. Osborne (eds.), *Diseases of the Breast*, 3rd edn., Philadelphia, PA: Lippincott Williams & Wilkins, pp. 1133–1142.

28. Hippocrates. 400 B.C. *The Book of Prognostics*. http://www.greektexts.com/library/Hippocrates/The_%20Book_Of_Prognostics/eng/4.html AQ3

29. Itoh, A., E. Ueno, E. Tohno, H. Kamma, H. Takahashi, T. Shiina, M. Yamakawa, and T. Matsumura. 2006. Breast disease: Clinical application of US elastography for diagnosis. *Radiology* **9**:341–350.

30. Johansson, J.E., O. Andrén, S.O. Andersson, P.W. Dickman, L. Holmberg, A. Magnuson, and H.O. Adami. 2004. Natural history of early, localized prostate cancer. *J. Amer. Med. Assoc*. **291**:2713–2719.

31. Johansson, R.S. and A.B. Vallbo. 1979. Tactile sensibility in the human hand: Relative and absolute densities of four types of mechanoreceptive units in glabrous skin. *J. Physiol*. **286**:283–300.

32. Kaufman, C.S., L. Jacobson, B. Bachman, and L. Kaufman. 2006. Digital documentation of the physical examination: Moving the clinical breast exam to the electronic medical record. *Am. J. Surg*. **192**:444–449.

33. Klotz, L. 2006. Active surveillance versus radical treatment for favorable risk localized prostate cancer. *Curr. Treat. Options Oncol*. **7**:355–362.

34. Kotani, K., S. Ito, T. Miura, and K. Horii. 2007. Evaluating tactile sensitivity adaptation by measuring the differential threshold of archers. *J. Physiol. Anthropol.* **26**:143–148.

35. Krouskop, T.A., T.M. Wheeler, F. Kallel, B.S. Garra, and T. Hall. 1998. Elastic moduli of breast and prostate tissues under compression. *Ultrason. Imaging* **20**:260–274.

36. Laxminarayan, R., J. Chow, and S.A. Shahid-Salles. 2006. Intervention cost-effectiveness: Overview of main messages. In D.T. Jamison, J.G. Breman et al. (eds.), *Disease Control Priorities in Developing Countries*, 2nd edn., Washington, DC: Oxford University Press, pp. 35–86.

37. Lederman, S.J. and R.L. Klatzky. 2009. Human haptics. In L.R. Squire (ed. in Chief), *Encyclopedia of Neuroscience*, vol. 5. San Diego, CA: Academic Press, pp.11–18.

38. Lee, H.K., S.I. Chang, and E. Yoon. 2006. A flexible polymer tactile sensor: Fabrication and modular expandability for large area deployment. *J. Microel. Systems* **15**:1681–1686.

39. Lee, M.H. and H.R. Nichols. 1999. Tactile sensing for mechatronics: A state of the art survey. *Mechatronics* **9**:1–31.

40. Liang, W., W.F. Lawrence, C.B. Burnett, Y.T. Hwang, M. Freedman, B.J. Trock, J.S. Mandelblatt, and M.E. Lippman. 2003. Acceptability of diagnostic tests for breast cancer. *Breast Cancer Res. Treat.* **79**:199–206.

41. Libouton, X., O. Barbier, L. Plaghki, and J.L. Thonnard. 2010. Tactile roughness discrimination threshold is unrelated to tactile spatial acuity. *Behav. Brain. Res.* **208**:473–478.

42. Mei, T., W.J. Li, Y. Ge, Y. Chen, L. Ni, and M.N. Chan. 2000. An integrated MEMS three-dimensional tactile sensor with large force range. *Sens. Actuat. A Phys.* **80**:155–162.

43. Multhupillai, R., D.J. Lomas, P.J. Rossman, J.F. Greenleaf, A. Manduca, and R.L. Ehman. 1995. Magnetic resonance elastography by direct visualization of propagating acoustic strain waves. *Science* **269**:1854–1857.

44. Niemczyk, P., A.P. Sarvazyan, A. Fila, P. Amenta, W.S. Ward, P. Javidian, K. Breslayer, and K.B. Cummings. 1996. Mechanical imaging, a new technology for prostate cancer detection. *Surg. Forum* **47**:823–825.

45. Niemczyk, P., K.B. Cummings, A.P. Sarvazyan, E. Bancila, W.S. Ward, and R.E. Weiss. 1998. Correlation of mechanical imaging and histopathology of radical prostatectomy specimens: A pilot study for detecting prostate cancer. *J. Urol.* **160**:797–801.

46. Nightingale, K., M.S. Soo, R. Nightingale, and G. Trahey. 2002. Acoustic radiation force impulse imaging: In vivo demonstration of clinical feasibility. *Ultrasound Med. Biol.* **28**:227–235.

47. Ophir, J., I. Cespedes, H. Ponnekanti, Y. Yazdi, and X. Li. 1991. Elastography: A quantitative method for imaging the elasticity of biological tissues. *Ultrason. Imaging* **13**:111–134.

48. Ohnuki, K., S. Kuriyama, N. Shoji, Y. Nishino, I. Tsuji, and N. Ohuchi. 2006. Cost-effectiveness analysis of screening modalities for breast cancer in Japan with special reference to women aged 40–49 years. *Cancer Sci.* **97**:1242–1247.

49. Parker, C. 2004. Active surveillance: Towards a new paradigm in the management of early prostate cancer. *Lancet Oncol.* **5**:101–106.

50. Parker, K.J., S.R. Huang, R.A. Musulin, and R.M. Lerner. 1990. Tissue response to mechanical vibrations for "sonoelasticity imaging." *Ultrasound Med. Biol.* **16**:241–246.

51. Patel, M.I., D.T. DeConcini, E. Lopez-Corona, M. Ohori, T. Wheeler, and P.T. Scardino. 2004. An analysis of men with clinically localized prostate cancer who deferred definitive therapy. *J. Urol.* **171**:1520–1524.

52. Plewes, D.B., I. Betty, S.N. Urchuk, and I. Soutar. 1995. Visualizing tissue compliance with MR imaging. *J. Mag. Res. Imaging* **5**:733–738.

AQ4
53. Pressure mapping and force measurement. Sensor technology. http://www.tekscan.com/technology.html#1

54. Raza, S., A. Odulate, E.M. Ong, S. Chikarmane, and C.W. Harston. 2010. Using real-time tissue elastography for breast lesion evaluation: Our initial experience. *J. Ultrasound Med.* **29**:551–563.

55. Russell, R.A. 2002. A tactile sensor skin for measuring surface contours. In *Proceedings of IEEE Region 10 International Conference on Technology Enabling Tomorrow: Computers, Communications and Automation towards the 21st Century,* Melbourne, Victoria, Australia, pp. 262–266.

56. Russell, R.A. and S. Parkinson. 1993. Sensing surface shape by touch. In *Proceedings of IEEE International Conference on Robotics and Automation,* Atlanta, GA, pp. 423–428.

57. Sabatini, A.M., P. Dario, and M. Bergamasco. 1990. Interpretation of mechanical properties of soft tissues from tactile measurements. In *Lecture Notes in Control and Information Sciences*, vol. 139. *The First International Symposium on Experimental Robotics*, Springer-Verlag, London, U.K., pp. 452–462.

58. Sarvazyan, A.P. 1998. Mechanical imaging: A new technology for medical diagnostics. *Int. J. Med. Inf*. **49**:195–216.

59. Sarvazyan, A.P. 1998. Computerized palpation is more sensitive than human finger. In *Proceedings of the 12th International Symposium on Biomedical Measurements and Instrumentation*, Dubrovnik, Croatia, pp. 523–524.

60. Sarvazyan, A.P. 2001. Elastic properties of soft tissues. In M. Levy, H.E. Bass, R.R. Stern (eds.), *Handbook of Elastic Properties of Solids, Liquids and Gases,* vol. III, Chapter 5, New York: Academic Press, pp. 107–127.

61. Sarvazyan, A.P. 2006. Tissue viscoelasticity: Past and future, unexplored areas and brave projections. In *Proceedings of the 5th International Conference on the Ultrasonic Measurement and Imaging of Tissue Elasticity*, Snowbird, UT.

62. Sarvazyan, A.P., V. Egorov, J.S. Son, and C.S. Kaufman. 2008. Cost-effective screening for breast cancer worldwide: Current state and future directions. *Breast Cancer: Basic Clin. Res*. **1**:91–99.

63. Sarvazyan, A.P. and A.R. Skovoroda. June 1996. Method and apparatus for elasticity imaging. U.S. patent 5,524,636.

64. Sarvazyan, A.P., A.R. Skovoroda, S.Y. Emelianov, J.B. Fowlkes, J.G. Pipe, R.S. Adler, R.B. Buxton, and P.L. Carson. 1995. Biophysical bases of elasticity imaging. In J.P. Jones (ed.), *Acoustical Imaging*, vol. 21, New York: Plenum Press, pp. 223–240.

65. Sarvazyan, A.P., O.V. Rudenko, S.D. Swanson, J.B. Fowlkes, and S.Y. Emelianov. 1998. Shear wave elasticity imaging: A new ultrasonic technology of medical diagnostics. *Ultrasound Med. Biol*. **24**:1419–1435.

66. Saslow, D., C. Boetets, W. Burke, S. Harms, M.O. Leach, C.D. Lehman, E. Morris, E. Pisano, M. Schnall, S. Sener, R.A. Smith, E. Warner, M. Yaffe, K.S. Andrews, C.A. Russell, and American Cancer Society Breast Cancer Advisory Group. 2007. American Cancer Society guidelines for breast screening with MRI as an adjunct to mammography. *CA Cancer J. Clin*. **57**:75–89.

67. Sathian, K., A. Zangaladze, J. Green, J.L. Vitek, and M.R. DeLong. 1997. Tactile spatial acuity and roughness discrimination: Impairment due to aging and Parkinson's disease. *Neurology* **49**:168–177.

68. Sinkus, R., J. Lorenzen, D. Schrader, M. Lorenzen, M. Dargatz, and D. Holz. 2000. High-resolution tensor MR elastography for breast tumour detection. *Phys. Med. Biol*. **45**:1649–1664.

69. Sinkus, R., K. Siegmann, M. Tanter, T. Xydeas, and M. Fink. 2007. MR–elastography is capable of increasing the specificity of MR-mammography influence of rheology on the diagnostic gain. In *Proceedings of the 6th International Conference on the Ultrasonic Measurement and Imaging of Tissue Elasticity*, Snowbird, UT, p. 111.

70. Skovoroda, A.R., A.N. Klishko, D.A. Gusakian, E.I. Maevskii, V.D. Ermilova, G.A. Oranskaia, and A.P. Sarvazyan. 1995. Quantitative analysis of the mechanical characteristics of pathologically changed biological tissues. *Biophysics* **40**:1359–1364.

71. Son, J.S. and T. Parks. October 2008. Hybrid tactile sensor. U.S. patent 7,430,925.

72. Svensson, W.E., N. Zaman, N.K. Barrett, G. Ralleigh, K. Satchithananda, S. Comitis, V. Gada, and N.R. Wakeham. 2007. Breast elasticity imaging aids patient management in the one stop breast clinic. In *Proceedings of the 6th International Conference on the Ultrasonic Measurement and Imaging of Tissue Elasticity*, Santa Fe, NM, p. 128.

73. Tegin, J. and J. Wikander. 2005. Tactile sensing in intelligent robotic manipulation—A review. *Ind. Rob*. **32**:64–70.

74. Thomas, A., T. Fischer, H. Frey, R. Ohlinger, S. Grunwald, J.U. Blohmer, K.J. Winzer, S. Weber, G. Kristiansen, B. Ebert, and S. Kümmel. 2006. Real-time elastography—An advanced method of ultrasound: First results in 108 patients with breast lesions. *Ultrasound Obstet. Gynecol*. **28**:335–340.

75. Tosteson, A.N., N.K. Stout, D.G. Fryback, S. Acharyya, B.A. Herman, L.G. Hannah, E.D. Pisano, and DMIST Investigators. 2008. Cost-effectiveness of digital mammography breast cancer screening. *Ann. Int. Med*. **148**:1–10.

76. Wellman, P.S. 1999. Tactile imaging. PhD thesis. Harvard University's Division of Engineering and Applied Sciences, Cambridge, MA.

77. Wellman, P.S., E.P. Dalton, D. Krag, K.A. Kern, and R.D. Howe. 2001. Tactile imaging of breast masses: First clinical report. *Arch. Surg*. **136**:204–208.

78. Weiss, R., V. Egorov, S. Ayrapetyan, N. Sarvazyan, and A.P. Sarvazyan. 2008. Prostate mechanical imaging: A new method for prostate assessment. *Urology* **71**:425–429.

79. Weiss, R., V. Hartanto, M. Perrotti, K. Cummings, A. Bykanov, V. Egorov, and S.A. Sobolevsky. 2001. In vitro trial of the pilot prototype of the prostate mechanical imaging system. *Urology* **58**:1059–1163.
80. Wolfe, J.M., K.R. Kluender, D.M. Levi, L.M. Bartoshuk, R.S. Herz, R.L. Klatzky, and S.J. Lederman. 2008. Touch. In *Sensation and Perception*, Chapter 12, 2nd edn., Sunderland, MA: Sinauer, pp. 286–313.
81. World Health Organization. February 2006. Fact sheet N 297. http://www.who.int/cancer/en/index.html
82. Zhi, H., X.Y. Xiao, H.Y. Yang, B. Ou, Y.L. Wen, and B.M. Luo. 2010. Ultrasonic elastography in breast cancer diagnosis strain ratio vs 5-point scale. *Acad. Radiol*. **17**:1227–1233.

AUTHOR QUERIES
[AQ1]   Please check the formatting of quote "…Such swellings…" for correctness.
[AQ2]   Please check if the sentence starting "Further, the ease-of-use,…" is ok.
[AQ3]   Please provide accessed date for Refs. [12,28,53,81].
[AQ4]   Please provide in-text citation for Ref. [53].